



Efficient blue and bluish-green iridium phosphors: Fine-tuning emissions of Flrpic by halogen substitution on pyridine-containing ligands



Cong Fan^a, Liping Zhu^b, Bei Jiang^a, Cheng Zhong^a, Dongge Ma^{b,*}, Jingui Qin^a, Chuluo Yang^{a,*}

^aHubei Collaborative Innovation Center for Advanced Organic Chemical Materials, Hubei Key Lab on Organic and Polymeric Optoelectronic Materials, Department of Chemistry, Wuhan University, Wuhan 430072, People's Republic of China

^bState Key Laboratory of Polymer Physics and Chemistry, Changchun Institute of Applied Chemistry, Chinese Academy of Sciences, Changchun 130022, People's Republic of China

ARTICLE INFO

Article history:

Received 26 July 2013

Received in revised form 12 September 2013

Accepted 14 September 2013

Available online 27 September 2013

Keywords:

Halogen atoms

Iridium compounds

Hammett parameters

Phosphorescent organic light-emitting diode

ABSTRACT

Three new iridium compounds, 4-F-Flrpic, 4-Cl-Flrpic and 4-Br-Flrpic, were designed and synthesized by introducing the F, Cl and Br atoms to the 4-position of pyridine ring in the frame of sky-blue emitter, Flrpic. Adding F atom stabilizes the HOMO level of Flrpic but keeps the LUMO level of Flrpic almost unchanged, which consequently broadens the HOMO–LUMO gap of Flrpic and finely tunes the emission to 465 nm of 4-F-Flrpic from 470 nm of Flrpic. In contrast, introducing of Cl and Br atoms simultaneously lowers the HOMO and LUMO levels of Flrpic, which brings about the squeeze of HOMO–LUMO gap in Flrpic and makes the emissions of 4-Cl-Flrpic and 4-Br-Flrpic red-shift to 475 and 479 nm, respectively. The phosphorescent organic light-emitting devices using the three iridium compounds as dopants were fabricated with the following configuration: ITO/MoO₃/TAPC/TCTA:dopants/Tm/LiF/Al. The device based on 4-F-Flrpic showed a blue emission with the Commission Internationale de L'Eclairage coordinate of (0.15, 0.28), and revealed rather high efficiencies, with maximum current efficiency of 29 cd A⁻¹, power efficiency of 29 lm W⁻¹ and external quantum efficiency of 14.6%.

© 2013 Elsevier B.V. All rights reserved.

1. Introduction

Phosphorescent organic light-emitting diodes (PhOLEDs) using organo-transition metal complexes as the phosphor dyes can harvest both electro-generated singlet and triplet excitons, achieving 100 % internal quantum efficiency [1]. Among the red-green-blue trichromatic emissions, blue light plays the indispensable role for achieving full-color displays and generating white light in combination with a complementary color for illumination [2]. However, the efficiencies and stabilities of blue PhOLEDs still need to be greatly improved [3]. To the present,

cyclometalated iridium (III) compounds are proved to be the most promising blue phosphor dyes due to their high phosphorescent quantum yield, microsecond-range lifetime and thermal stability among the organo-transition metal complexes [4].

Due to the spin–orbit coupling (SOC) and configuration interaction (CI), iridium (III) compounds exhibit sophisticated fine structures of electronic states [5,6]. The emissive lowest excited triplet state (T₁) is in fact nondegenerate and splitted into three substrates without the external magnetic field [7]. Each substrate possesses relatively individual radiative and non-radiative kinetic characteristics, depending on the degree of the contributions from the virtual excited singlet states mixed in each substrate for the CI effect [8]. These involved virtual excited singlet states would break the spin-forbidden transition and provide

* Corresponding authors. Tel.: +86 27 68756101 (C. Yang).

E-mail addresses: mdg1014@ciac.jl.cn (D. Ma), clyang@whu.edu.cn (C. Yang).

the allowedness of optical transitions to the electronic singlet ground state (S_0). As a result, modification on iridium compounds by introducing functional groups could disturb the fine electronic states and tune their photoluminescence (PL) emissions.

Based on the model of sky blue-emissive bis [2-(4',6'-difluoro)phenylpyridinato- N,C^2']iridium(III) picolinate (Flrpic) [9], some strategies are successfully adopted to broaden the gaps between the highest occupied molecular orbital (HOMO) and the lowest unoccupied molecular orbital (LUMO) of iridium (III) compounds to obtain blue emission, such as adding electron-donating groups ($-OMe$ [10], $-NMe_2$ [11]) to the pyridine moiety to elevate the LUMO level, or adding electron-withdrawing groups ($-F$ [12], $-CF_3$ [13], $-CN$ [14], $-COOMe$ [15], $-PO(-SO_2)$ [16]) to the phenyl moiety to pull down the HOMO level. Recently, Baranoff et al. demonstrated that the Hammett parameters would be useful to correlate the chemical structures of halogen-substituted phenyl rings to the electronic properties of Flrpic [17,18]. The HOMO and LUMO levels of Flrpic were differently affected by the inductive (σ_m) effect and resonance (σ_p) effect of halogen atoms. Interestingly, few studies report the employment of electron-withdrawing groups to the pyridine moiety, which are generally supposed to stabilize the LUMO level and consequently narrow the HOMO–LUMO gap of Flrpic.

In this article, we designed and synthesized three iridium compounds, 4-F-Flrpic, 4-Cl-Flrpic and 4-Br-Flrpic, by introducing fluorine, chlorine and bromine atoms to the 4-position of pyridine ring in the frame of Flrpic. The 4-F-Flrpic molecule exhibited blue-shift emission with peak emission at 465 nm compared to the 470 nm of Flrpic, whereas 4-Cl-Flrpic and 4-Br-Flrpic showed red-shift emissions with peak emission at 475 and 479 nm, respectively [19]. The analysis of cyclic voltammetry and quantum chemistry calculations indicated that F atom decreased the HOMO level of Flrpic while kept the LUMO level of Flrpic almost undisturbed. The phosphorescent organic light-emitting device based on 4-F-Flrpic exhibited a blue emission with CIE coordinate of (0.15, 0.28), and revealed rather high efficiencies, with maximum current efficiency of 29 cd A $^{-1}$, power efficiency of 29 lm W $^{-1}$ and external quantum efficiency of 14.6%.

2. Experimental section

2.1. General information

All reactions were carried out using Schlenk tube in an argon atmosphere. All reagents commercially available were used as received unless otherwise stated. The solvents (tetrahydrofuran, diethyl ether, dichloromethane) were purified by conventional procedure and distilled under argon before using. 1H NMR spectra were measured on Varian Unity 300 MHz spectrometer using $CDCl_3$ as solvent and tetramethylsilane as an internal reference. ^{13}C NMR (75 MHz) spectra were measured on Varian Unity 300 MHz spectrometer using $CDCl_3$ as solvent. The chemical shifts reported for the ^{13}C NMR spectra reflected the positions of the observed peaks at the frequency given,

some of which were expected to arise due to coupling to ^{19}F , and these couplings had not been assigned. Elemental analysis of carbon, hydrogen and nitrogen was performed on Vario EL-III microanalyzer. EI-MS spectra were recorded on VJ-ZAB-3F-Mass spectrometer. Thermogravimetric analysis (TGA) was undertaken with a NETZSCH STA 449C instrument and the thermal stability of the samples under nitrogen atmosphere was determined by measuring their weight loss, heated at a rate of 10 °C min $^{-1}$ from 25 °C to 600 °C.

2.2. Photophysical characterization

UV–vis absorption spectra were recorded on Shimadzu UV-2550 spectrophotometer with baseline corrected. Steady-state emission spectra were recorded on Hitachi F-4500 fluorescence spectrophotometer. Absolute photoluminescence quantum yields measured in CH_2Cl_2 were recorded on FLS920 spectrometer with Xenon light source (450 W) through the Edinburgh Instruments integrating sphere. The integrating sphere is 150 mm in diameter and has its inner surface coated with Barium Sulfate ($BaSO_4$). Time-resolved measurements in CH_2Cl_2 solution were performed on FLS920 spectrometer using the time-correlated single-photon counting (TCSPC) option and the Edinburgh Instruments picoseconds pulsed diode laser (Model: EPL-375) as the light source. The excited state lifetime data were analyzed using F900 software by minimizing the reduced chi squared function (χ^2) and visual inspection of the weighted residuals. After collecting the data, a lifetime value in the window of the F900 software was initially given, then the F900 software will automatically get a analyzed lifetime value and a corresponding value of the reduced chi squared function (χ^2). When the given value of χ^2 is in the range of 1.0–1.2, the analyzed lifetime value of the iridium complex is supposed to be well fitted. All the samples were fresh and carefully prepared. Deaerated samples were prepared by purging argon for 60 min.

2.3. Cyclic voltammetry

Cyclic voltammetric measurements were carried out by using a CHI voltammetric analyzer. Tetrabutylammonium hexafluorophosphate (0.1 M) was used as the supporting electrolyte. The conventional three-electrode cell with a Pt work electrode of 2 mm diameter, a platinum-wire counter electrode and a Ag/AgCl reference electrode was employed. The scan rate is 0.1 V s $^{-1}$. At the end of each experiment, the ferrocene/ferricenium (Fc/Fc^+) couple was used as the internal standard. The HOMO and LUMO energy levels (eV) of the four compounds are calculated according to the formula: $-[4.8 \text{ eV} + (E_{1/2(\text{reversible})})E_{\text{onset}}(\text{irreversible}) - E_{1/2(\text{Fc/Fc}^+)})]$.

2.4. Theoretical calculations

The geometrical and electronic properties of all the four iridium compounds were carried out with the Gaussian 09 package [20]. All the geometries were optimized at B3LYP/cc-pVDZ level with cc-pVDZ-pp pseudo potential on iridium (III) metal. Then the time-dependent density

functional theory (TD-DFT) was used to calculate their triplet state energies and a subsequent nature transition orbital (NTO) analysis was used to visualize the triplet state distribution.

2.5. Device fabrication and measurement

The sky-blue Flrpic, hole-injection material MoO₃, hole-transporting material 1,1-bis[(di-4-tolylamino)phenyl]cyclohexane (TAPC), host material 4,4',4''-tris(carbazol-9-yl)-triphenylamine (TCTA) and electron-transporting material 1,3,5-tri(*m*-pyrid-3-yl-phenyl) benzene (Tm) were commercially available. The three iridium complexes were purified by crystallization in CH₂Cl₂/hexane solution. Commercial indium tin oxide (ITO) coated glass with sheet resistance of 10 Ω/square was used as the starting substrates. Before device fabrication, the ITO glass substrates were pre-cleaned carefully and treated by UV/O₃ for 2 min. Then the sample was transferred to the deposition system. 10 nm of MoO₃ was firstly deposited to ITO substrates, followed by 60 nm TAPC, 20 nm emissive layer and 30 nm Tm. Finally, a cathode composed of 1 nm of lithium fluoride and 120 nm of aluminum was sequentially deposited onto the substrates in the vacuum of 10⁻⁶ Torr to construct the devices. In the deposition of the emissive layer, the host and guest were placed into different evaporator sources. The deposition rates of both host and guest were controlled with their correspondingly independent quartz crystal oscillators. The evaporation rates were monitored by a frequency counter and calibrated by a Dektak 6M profiler (Veeco). The I–V–B of all devices was measured with a Keithley 2400 Source meter and a Keithley 2000 Source multimeter equipped with a calibrated silicon photodiode. The electroluminescence (EL) spectra were measured by JY SPEX CCD3000 spectrometer. All measurements were carried out at room temperature under ambient conditions.

2.5.1. Synthesis of 2-(2',4'-difluorophenyl)-4-fluoropyridine (4-F-dfppy)

A mixture of 2-chloro-4-fluoropyridine (0.66 g, 5 mmol), 2,4-difluorophenylboronic acid (0.79 g, 5 mmol), Pd(OAc)₂ (0.023 g, 0.1 mmol), PPh₃ (0.105 g, 0.4 mmol) and K₂CO₃ (1.1 g, 8 mmol) in 10 ml of 1,2-dimethoxyethane was refluxed at 80 °C for 12 h under argon atmosphere. After cooled to room temperature, the mixture was poured into water, extracted with CHCl₃ and dried over anhydrous Na₂SO₄. The product was purified by column chromatography on silica gel using 1: 10 (v:v) ethyl acetate/petroleum as eluent to give a white solid. Yield: 50%. ¹H NMR (300 MHz, CDCl₃) δ [ppm]: 8.68–8.63 (m, 1H), 8.10–8.02 (m, 1H), 7.51 (d, *J* = 10.2 Hz, 1H), 7.03–6.88 (m, 3H). ¹³C NMR (75 MHz, CDCl₃) δ [ppm]: 170.34, 166.88, 165.05, 164.89, 162.25, 162.10, 161.71, 161.55, 158.89, 158.74, 154.87, 151.51, 151.43, 131.97, 131.90, 122.36, 111.75, 111.60, 111.50, 111.36, 110.02, 109.80, 104.46, 104.11, 103.76. MS (EI, *m/z*): [M]⁺ calcd for C₁₁H₆F₃N, 209.05; found, 209.03. Anal. calcd for C₁₁H₆F₃N (%): C 63.16, H 2.89, N 6.70; found: C 63.35, H 3.01, N 6.95.

2.5.2. Synthesis of 2-(2',4'-difluorophenyl)-4-chloropyridine (4-Cl-dfppy)

The procedure is same as 4-F-dfppy by using 2,4-dichloropyridine as the reagent. Yield: 70%. ¹H NMR (300 MHz, CDCl₃) δ [ppm]: 8.50 (d, *J* = 5.1 Hz, 1H), 7.97–7.89 (m, 1H), 7.69 (s, 1H), 7.19–7.17 (m, 1H), 6.95–6.80 (m, 2H). ¹³C NMR (75 MHz, CDCl₃) δ [ppm]: 165.12, 164.97, 162.24, 162.07, 161.79, 161.62, 158.87, 158.72, 153.56, 150.20, 144.27, 132.08, 132.01, 124.19, 124.05, 122.46, 111.99, 111.71, 104.62, 104.29, 103.93. MS (EI, *m/z*): [M]⁺ calcd for C₁₁H₆ClF₂N, 225.02; found, 225.01. Anal. calcd for C₁₁H₆ClF₂N (%): C 58.56, H 2.68, N 6.21; found: C 58.47, H 2.54, N 6.40.

2.5.3. Synthesis of 2-(2',4'-difluorophenyl)-4-bromopyridine (4-Br-dfppy)

A mixture of 2,4-dibromopyridine (7.1 g, 30 mmol), 2,4-difluorophenylboronic acid (4.7 g, 30 mmol), Pd(PPh₃)₄ (22 mg, 5% mmol), Na₂CO₃ (3.8 g, 36 mmol) in 20 ml of tetrahydrofuran (THF) and 5 ml of distilled water was refluxed for 2 days under argon. The mixture was extracted with CHCl₃ and dried over anhydrous Na₂SO₄. The product was purified by column chromatography on silica gel using 1: 10 (v:v) ethyl acetate/petroleum as eluent to give a white solid. Yield: 30%. ¹H NMR (300 MHz, CDCl₃) δ [ppm]: 8.49 (d, *J* = 5.1 Hz, 1H), 8.02–7.91 (m, 2H), 7.41–7.39 (m, 1H), 7.01–6.86 (m, 2H). ¹³C NMR (75 MHz, CDCl₃) δ [ppm]: 165.13, 164.97, 162.20, 162.04, 161.79, 161.62, 158.69, 153.47, 150.10, 133.01, 132.11, 132.03, 127.19, 127.05, 125.48, 122.31, 122.16, 112.01, 111.73, 104.67, 104.33, 103.98. MS (EI, *m/z*): [M]⁺ calcd for C₁₁H₆BrF₂N, 268.97; found, 268.98. Anal. calcd for C₁₁H₆BrF₂N (%): C 48.92, H 2.24, N 5.19; found: C 49.01, H 2.04, N 5.22.

2.5.4. Synthesis of 4-F-Flrpic

A mixture of 2.5 equiv of 2-(2',4'-difluorophenyl)-4-fluoropyridine (4-F-dfppy, 0.53 g, 2.5 mmol) and 1 equiv of IrCl₃·3H₂O (0.35 g, 1 mmol), 15 ml of 2-ethoxyethanol and 5 ml of H₂O was refluxed at 120 °C for 24 h under an argon atmosphere. After back to room temperature, the mixture was poured into water and the formed precipitate was filtered, washed by water, ethanol and diethyl ether to obtain the intermediate, assumed to be a chloro-bridged dimer. Without further purification, a mixture of the intermediate (0.39 g, 0.3 mmol), Na₂CO₃ (0.32 g, 3 mmol), and picolinic acid (0.19 g, 1.5 mmol) was added into 20 ml 1, 2-dichloroethane solvent. The reaction was refluxed at 80 °C for 12 h under an argon atmosphere, then extracted with CH₂Cl₂ and dried over anhydrous Na₂SO₄. The product was obtained by column chromatography on silica gel using 1: 10 (v:v) ethanol/CH₂Cl₂ as eluent to give a yellow solid. Overall yields: 40%. ¹H NMR (300 MHz, CDCl₃) δ [ppm]: 8.70 (t, *J* = 6.9 Hz, 1H), 8.35 (d, *J* = 7.8 Hz, 1H), 8.03–7.94 (m, 3H), 7.77 (d, *J* = 4.8 Hz, 1H), 7.47 (t, *J* = 6.3 Hz, 1H), 7.36 (t, *J* = 6.6 Hz, 1H), 7.02–6.96 (m, 1H), 6.80–6.75 (m, 1H), 6.55–6.40 (m, 2H), 5.86–5.83 (m, 1H), 5.60–5.56 (m, 1H). ¹³C NMR (75 MHz, CDCl₃) δ [ppm]: 172.75, 171.52, 168.66, 167.29, 165.24, 164.83, 162.92, 162.64, 162.51, 160.73, 153.08, 151.99, 150.90, 150.36, 148.58, 138.89, 128.92, 127.82, 127.69, 115.13, 114.85, 114.17, 111.57, 111.16, 110.89, 99.28, 99.15, 98.87, 98.60,

98.19. MS (EI, m/z): $[M]^+$ calcd for $C_{28}H_{14}F_6IrN_3O_2$, 731.06; found, 731.01. Anal. calcd for $C_{28}H_{14}F_6IrN_3O_2$ (%): C 46.03, H 1.97, N 5.57; found: C 46.13, H 2.00, N 5.62.

2.5.5. Synthesis of 4-Cl-Flrpic

The procedure is the same as the synthesis of 4-F-Flrpic by using 2-(2',4'-difluorophenyl)-4-chloropyridine (0.56 g, 2.5 mmol) as the ligand. Overall yields: 56%. 1H NMR (300 MHz, $CDCl_3$) δ [ppm]: 8.61 (d, $J = 6.6$ Hz, 1H), 8.35–8.22 (m, 3H), 7.98 (t, $J = 7.5$ Hz, 1H), 7.73 (d, $J = 4.5$ Hz, 1H), 7.46 (t, $J = 6.9$ Hz, 1H), 7.29–7.19 (m, 2H), 6.99–6.97 (m, 1H), 6.54–6.39 (m, 2H), 5.84 (d, $J = 8.1$ Hz, 1H), 5.69 (d, $J = 8.4$ Hz, 1H). ^{13}C NMR (75 MHz, $CDCl_3$) δ [ppm]: 172.34, 166.52, 164.98, 163.14, 152.66, 151.11, 148.78, 148.06, 146.46, 138.55, 128.56, 127.01, 123.40, 123.11, 122.91, 122.71, 122.53, 114.71, 114.48, 114.24, 98.62, 98.28, 97.92, 97.57. MS (EI, m/z): $[M]^+$ calcd for $C_{28}H_{14}Cl_2F_4IrN_3O_2$, 763.00; found, 763.08. Anal. calcd for $C_{28}H_{14}Cl_2F_4IrN_3O_2$ (%): C 44.04, H 1.85, N 5.50; found: C 44.12, H 1.88, N 5.42.

2.5.6. Synthesis of 4-Br-Flrpic

The procedure is the same as the synthesis of 4-F-Flrpic by using 2-(2',4'-difluorophenyl)-4-bromopyridine (0.67 g, 2.5 mmol) as the ligand. Overall yields: 70%. 1H NMR (300 MHz, $CDCl_3$) δ [ppm]: 8.53 (d, $J = 6.3$ Hz, 1H), 8.44–8.33 (m, 3H), 7.98 (t, $J = 6.6$ Hz, 1H), 7.73 (d, $J = 4.8$ Hz, 1H), 7.47 (t, $J = 6.0$ Hz, 1H), 7.34 (d, $J = 5.1$ Hz, 1H), 7.19 (d, $J = 6.3$ Hz, 1H), 7.13–7.12 (m, 1H), 6.55–6.40 (m, 2H), 5.86 (d, $J = 6.9$ Hz, 1H), 5.60 (d, $J = 6.6$ Hz, 1H). ^{13}C NMR (75 MHz, $CDCl_3$) δ [ppm]: 165.46, 152.98, 151.77, 149.08, 148.39, 148.27, 138.94, 135.56, 129.01, 126.93, 126.64, 126.40, 126.12, 125.93, 114.95, 114.71, 98.74, 98.38, 98.02. MS (EI, m/z): $[M]^+$ calcd for $C_{28}H_{14}Br_2F_4IrN_3O_2$, 850.90; found, 850.68. Anal. calcd for $C_{28}H_{14}Br_2F_4IrN_3O_2$ (%): C 39.45, H 1.66, N 4.93; found: C 39.80, H 1.71, N 5.01.

3. Results and discussion

3.1. Synthesis and characterization

The synthesis of the ligands, 2-(2',4'-difluorophenyl)-4-fluoropyridine (4-F-dfppy), 4-chloro-2-(2',4'-difluorophenyl)pyridine (4-Cl-dfppy) and 4-bromo-2-(2',4'-difluorophenyl)pyridine (4-Br-dfppy) was depicted in Scheme 1. 4-F-dfppy and 4-Cl-dfppy were obtained by a modified Suzuki cross coupling reaction between 2-chloro-4-fluoropyridine/2,4-dichloropyridine and 2,4-difluorophenyl boronic acid [10]. 4-Br-dfppy was separated from the Suzuki cross coupling reaction between 2,4-dibromopyridine and 2,4-difluorophenyl boronic acid. The three iridium compounds were prepared in a conventional two-step procedure, as shown in Scheme 2 [21]. All the compounds were fully characterized by 1H and ^{13}C NMR spectroscopy, mass spectrum and elemental analysis (see details in Section 2). The thermal decomposition temperatures of the three iridium compounds (T_d , corresponding to 5% weight loss in the thermogravimetric analysis) were in the range of 340–360 °C (Fig. S1), indicating satisfactory thermal stabilities.

3.2. Photophysical properties

The UV–vis absorption and photoluminescence spectra of 4-F-Flrpic, 4-Cl-Flrpic and 4-Br-Flrpic in CH_2Cl_2 solution were shown in Fig. 1. In general, the intense short wavelength absorptions between 250 and 350 nm were due primarily to the spin-allowed $\pi-\pi^*$ transitions of the ligands, while the weak long wavelength absorptions between 400 and 460 nm could be assigned to the admixture of 1MLCT and 3MLCT transitions [6]. The three iridium compounds showed intense photoluminescence emission in CH_2Cl_2 solution at room temperature. 4-F-Flrpic molecule exhibited small blue-shift emission compared to Flrpic (470, 489 nm) with the maximum emissions at 465 and 487 nm [19], which was contrary to the common view that the electron-withdrawing F atom attaching on pyridine ring should bring down the LUMO level and subsequently narrow the HOMO–LUMO energy gap. On the other hand, 4-Cl-Flrpic and 4-Br-Flrpic molecules manifested red-shift photoluminescence spectra with the maximum emissions at 475, 501 nm and 479, 501 nm, respectively. Their absolute photoluminescence quantum yields (PLQYs) measured in deaerated CH_2Cl_2 solution were 40% for 4-F-Flrpic, 67% for 4-Cl-Flrpic and 59% for 4-Br-Flrpic. Under the same conditions, the value was 50% for Flrpic. The photo-excited decay curves of the three iridium compounds were shown in Fig. 2. Their fitting lifetimes were calculated to be 0.47 μs (4-F-Flrpic), 0.51 μs (4-Cl-Flrpic) and 0.44 μs (4-Br-Flrpic), respectively, which were almost monoexponential and indicated the triplet nature of excited states [22]. All the thermal and photophysical data of 4-F-Flrpic, 4-Cl-Flrpic and 4-Br-Flrpic were summarized in Table 1.

3.3. Electrochemical properties

The electrochemical behaviors of 4-F-Flrpic, 4-Cl-Flrpic and 4-Br-Flrpic were examined by the cyclic voltammetry (CV) using Fc/Fc^+ couple as the internal standard. For comparison, the electrochemical behaviors of Flrpic were measured under the same conditions. As shown in Fig. 3, all four iridium compounds exhibited reversible oxidation process in CH_2Cl_2 solution. The half-wave oxidation potentials (E_{ox} versus Fc/Fc^+) were 0.90 V (Flrpic), 1.02 V (4-F-Flrpic), 1.03 V (4-Cl-Flrpic) and 1.02 V (4-Br-Flrpic), respectively. Consequently, their HOMO energy levels determined from the half-wave oxidation potentials were -5.70 eV (Flrpic), -5.82 eV (4-F-Flrpic), -5.83 eV (4-Cl-Flrpic) and -5.82 eV (4-Br-Flrpic), respectively. For the reduction behaviors in deaerated THF solution, Flrpic and 4-F-Flrpic exhibited reversible behaviors, whereas 4-Cl-Flrpic and 4-Br-Flrpic exhibited irreversible behaviors. The reduction potentials (E_{red} versus Fc/Fc^+) estimated from the reduction onsets were -2.41 V (Flrpic), -2.40 V (4-F-Flrpic), -2.25 V (4-Cl-Flrpic) and -2.12 V (4-Br-Flrpic), respectively. Accordingly, their LUMO energy levels were -2.39 eV (Flrpic), -2.40 eV (4-F-Flrpic), -2.55 eV (4-Cl-Flrpic) and -2.68 eV (4-Br-Flrpic). Noticeably, F, Cl and Br atoms all lowered the HOMO level of Flrpic. However, adding F atom made LUMO level of Flrpic nearly invariant, but Cl and Br atoms both stabilized the LUMO level. These data were listed in Table 2.

Table 1

Thermal and photophysical properties of 4-F-Flrpic, 4-Cl-Flrpic and 4-Br-Flrpic.

Compounds	T_d (°C)	$\lambda_{\text{absmax}}^a$ (nm) ($\epsilon \times 10^3$)	λ_{PLmax}^a (nm)	Φ (%) ^b	τ_{obs}^b (μs)
4-F-Flrpic	362	259 (66.3), 383 (6.7)	465, 487	40	0.47
4-Cl-Flrpic	357	262 (83.8), 386 (10.6)	475, 501	67	0.51
4-Br-Flrpic	344	263 (60.5), 385 (8.0)	479, 501	59	0.44

^a Measured in CH_2Cl_2 solution (extinction coefficient in parentheses).^b Φ = absolute photoluminescence quantum yields in deaerated CH_2Cl_2 ; τ_{obs} = excited-state lifetimes.

3.4. DFT calculations

The calculated HOMO and LUMO orbital distributions of Flrpic, 4-F-Flrpic, 4-Cl-Flrpic and 4-Br-Flrpic were shown in Fig. 4. The HOMO orbitals of 4-F-Flrpic, 4-Cl-Flrpic and 4-Br-Flrpic involved the participation of π -orbitals from the pyridine rings, which indicated the F, Cl and Br atoms would affect the HOMO energy levels. The calculated values of HOMO/LUMO levels, energy gaps and triplet energies for the four iridium compounds were summarized in Tab. 2. Compared to the HOMO of Flrpic (ca. -5.57 eV), the replacement of H atom by F, Cl and Br atoms significantly lowered the HOMO level to ca. -5.72 eV (F), -5.76 eV (Cl) and -5.75 eV (Br). Meanwhile, the F, Cl and Br atoms lowered the LUMO level of Flrpic (ca. -1.93 eV) as well, but Cl (ca. -2.19 eV) and Br (ca. -2.20 eV) atoms stabilized the LUMO more than the F atom (ca. -2.02 eV). Consequently, the energy gap of 4-F-Flrpic (ca. 3.70 eV) was wider than Flrpic (ca. 3.64 eV), but 4-Cl-Flrpic (ca. 3.57 eV) and 4-Br-Flrpic (ca. 3.55 eV) displayed narrowed energy gaps. The calculated triplet energy of 4-F-Flrpic (ca. E_T 2.75 eV) was the highest among the four iridium compounds, while the triplet energies of 4-Cl-Flrpic (ca. E_T 2.68 eV) and 4-Br-Flrpic (ca. E_T 2.67 eV) were lower than the triplet energy of Flrpic (ca. E_T 2.70 eV).

The calculation results were in good accordance with the experimental results and can be interpreted by the inductive (σ_m) and resonance (σ_p) effects of halogen atom, which were quantitatively determined as the Hammett parameters [17]. As the Hammett parameters in Table 2 showed, the F, Cl and Br atoms were in *para*-position to the iridium (III) ion but *meta*-position to the 2,4-difluorophenyl ring. Due to the inductive (σ_m) effect to the 2,4-difluorophenyl ring, F, Cl and Br atoms would all stabilize the HOMO level of Flrpic. However, the H ($\sigma_p = 0$) and F

($\sigma_p = 0.06$) exhibited similar resonance effect on Flrpic, which indicated that substitutes from H to F would exert little influence on the electron density of iridium (III) ion. On the other hand, the Cl ($\sigma_p = 0.23$) and Br ($\sigma_p = 0.23$) still exhibited strong resonance effect to the Flrpic molecule, which consequently could bring in the stabilization of LUMO level in Flrpic.

3.5. Phosphorescent OLEDs

To evaluate the three new iridium compounds as the emissive dyes in phosphorescent organic light-emitting devices, we designed the following device structure: ITO/MoO₃ (10 nm)/TAPC (60 nm)/TCTA: 4-F-Flrpic (device A), 4-Cl-Flrpic (device B), 4-Br-Flrpic (device C) (20 nm)/Tm (30 nm)/LiF (1 nm)/Al (120 nm). For comparison, we also fabricated device D with Flrpic as the dopant. The device configuration was shown in Fig. 5. In these devices, MoO₃ and LiF served as hole- and electron-injecting materials; 1,1-bis[(di-4-tolylamino)phenyl]cyclohexane (TAPC) and 1,3,5-tri(*m*-pyrid-3-yl-phenyl)benzene (Tm) were used as hole- and electron-transporting materials, respectively; 4,4',4''-tris(carbazol-9-yl)-triphenylamine (TCTA) was employed as host material; the four iridium compounds were used as the guest emitters with optimized doping level at 10%. The current density–voltage–luminance (*J*–*V*–*L*) characteristics and current efficiency–power efficiency–EQE versus current density of all these devices were shown in Fig. 6. All the data were collected in Table 3.

As Fig. 6 revealed, the device B based on 4-Cl-Flrpic displayed the best performance among the four iridium compounds, with a turn-on voltage of 2.9 V, a maximum luminance of 13,482 cd m^{-2} , a maximum current efficiency of 39 cd A^{-1} , a maximum power efficiency of 41 lm W^{-1} , a maximum EQE of 16% and a CIE coordinate of (0.18, 0.40).

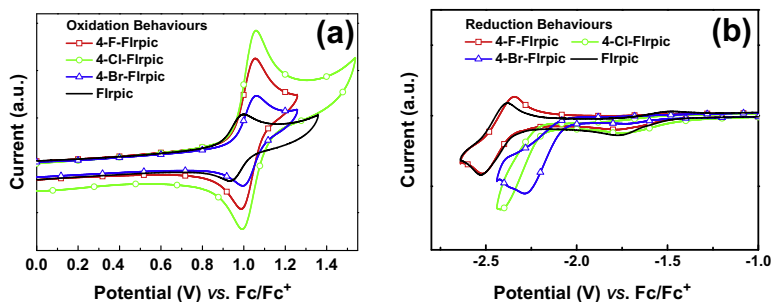


Fig. 3. Cyclic voltammogram of Flrpic, 4-F-Flrpic, 4-Cl-Flrpic and 4-Br-Flrpic versus Fc/Fc^+ couple: (a) oxidation behaviors in freshly distilled CH_2Cl_2 solution; (b) reduction behaviors in freshly distilled THF solution with oxygen removal.

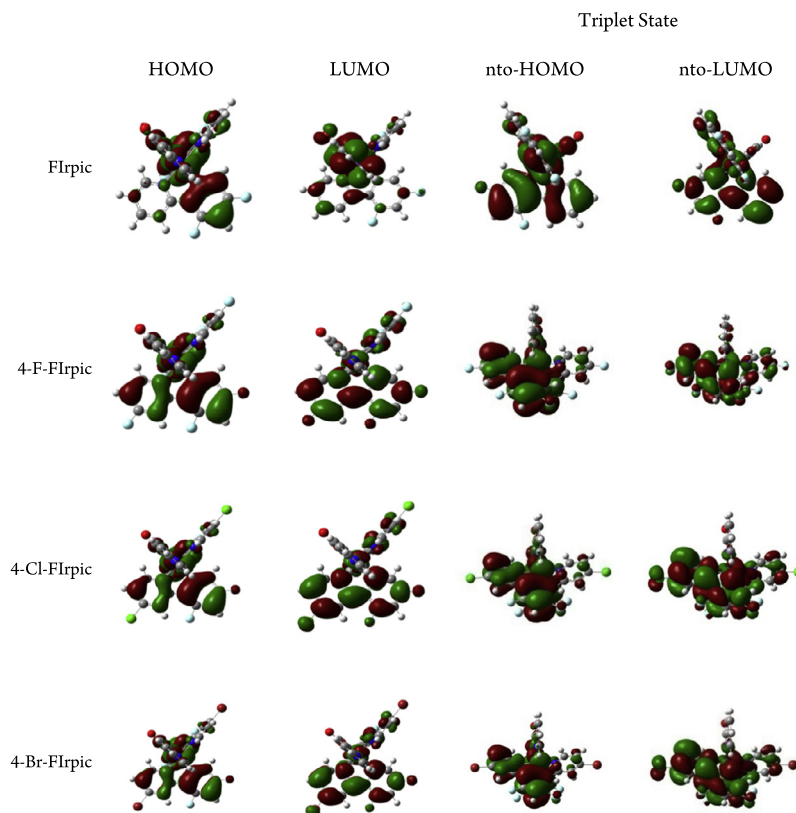


Fig. 4. Calculated HOMO/LUMO distributions of Flrpic, 4-F-Flrpic, 4-Cl-Flrpic and 4-Br-Flrpic, and their triplet states in nto-HOMO/nto-LUMO distribution.

Table 2

Calculated HOMO/LUMO, energy-gap and triplet-energy values of Flrpic, 4-F-Flrpic, 4-Cl-Flrpic and 4-Br-Flrpic.

	HOMO ^a (eV)	LUMO ^a (eV)	σ_m (meta to phenyl ring) ^b	σ_p (para to Ir) ^b	Computed HOMO (eV)	Computed LUMO (eV)	Computed energy gap (eV)	Computed triplet energy (eV)
Flrpic	-5.70	-2.39	0	0	-5.57	-1.93	3.64	2.70
4-F-Flrpic	-5.82	-2.40	0.34	0.06	-5.72	-2.02	3.70	2.75
4-Cl-Flrpic	-5.83	-2.55	0.37	0.23	-5.76	-2.19	3.57	2.68
4-Br-Flrpic	-5.82	-2.68	0.39	0.23	-5.75	-2.20	3.55	2.67

^a HOMO/LUMO energy levels determined from the oxidation/reduction potentials in the CV.

^b Hammett parameters cited from Ref. [17].

At practical brightness of 100 cd m^{-2} (0.40 mA cm^{-2} , 3.7 V), device B appeared current efficiency of 37 cd A^{-1} , power efficiency of 31 lm W^{-1} and EQE of 15.3%. At high brightness of 1000 cd m^{-2} (3.17 mA cm^{-2} , 4.7 V), device B still maintained high current efficiency of 30 cd A^{-1} , power efficiency of 20 lm W^{-1} and EQE of 12.5%. These efficiencies were better than the bluish-green iridium analogous reported in the literature [23]. The device C based on 4-Br-Flrpic exhibited fair performance, with a turn-on voltage of 3.1 V, a maximum current efficiency of 13 cd A^{-1} , a maximum power efficiency of 13 lm W^{-1} and external quantum efficiency (EQE) less than 5%. Compared to device B, the electroluminescence (EL) spectrum of device C displayed more strengthened shoulder emission around 501 nm than that of 4-Cl-Flrpic (see Supporting Information), which resulted in its red-shift CIE coordinate of

(0.26, 0.47). This also implicated that the exciton-combination zone in device C may be close to the metal cathode, and thus the excitons could be easily quenched by the triplet-polaron annihilation, consequently resulting in the low efficiency of device C [24].

The device A based on 4-F-Flrpic represented blue emission with CIE coordinate of (0.15, 0.28). Moreover, device A achieved satisfactory efficiencies with a maximum current efficiency of 29 cd A^{-1} , a maximum power efficiency of 29 lm W^{-1} and a maximum EQE of 14.6%. At practical brightness of 100 cd m^{-2} (0.41 mA cm^{-2} , 3.7 V), device A appeared current efficiency of 28 cd A^{-1} , power efficiency of 23 lm W^{-1} and EQE of 14%. At high brightness of 1000 cd m^{-2} (4.57 mA cm^{-2} , 4.9 V), device A still remained high current efficiency of 21 cd A^{-1} , power efficiency of 14 lm W^{-1} and EQE of 11%. The efficiencies of device

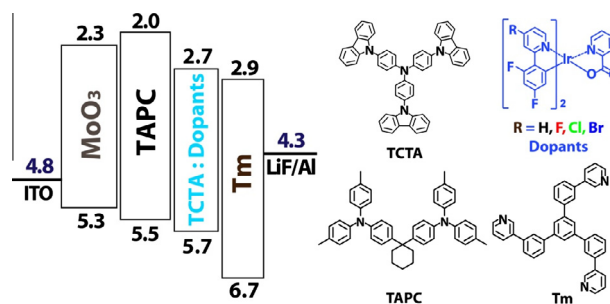


Fig. 5. The device configuration and chemical structures of used materials.

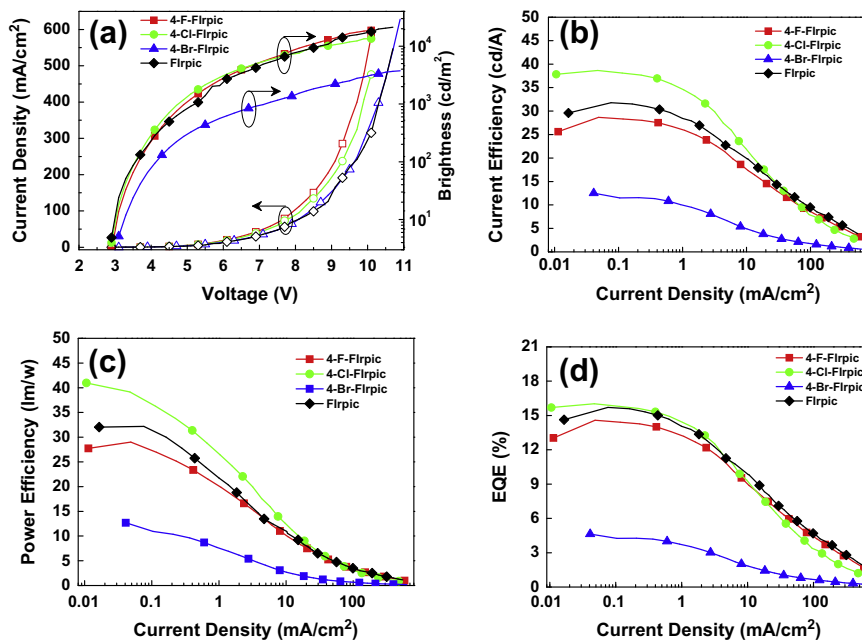


Fig. 6. (a) J - V - L characteristics of device A-D; (b) current efficiency versus current density of device A-D; (c) power efficiency versus current density of device A-D; (d) EQE versus current density of device A-D.

Table 3

Performance summary of device A-D.

Dopant	Device	V turn-on (V) ^a	L max (cd/m ²) ^b	EQE (%) ^c	LE (cd/A) ^c	PE (lm/W) ^c	CIE (x, y) ^d
4-F-Flrpic	A	2.9	18,773	14.6/14/11	29/28/21	29/23/14	(0.15, 0.28)
4-Cl-Flrpic	B	2.9	13,482	16/15.6/12.5	39/38/30	41/34/20	(0.18, 0.40)
4-Br-Flrpic	C	3.1	3745	4.6/3.8/1	13/10/2	13/8/2	(0.26, 0.47)
Flrpic	D	2.9	21,318	15.7/15.3/11.3	32/31/23	32/28/13	(0.15, 0.30)

^a Turn-on voltages at 1 cd m⁻².

^b Maximum luminance.

^c Order of measured efficiency values: maximum, then values at 100, 1000 cd m⁻² for device A-D.

^d Commission International de l'Eclairage (CIE) coordinates measured at 5 V.

A based on 4-F-Flrpic were comparable with the device D based on Flrpic, which displayed a maximum current efficiency of 32 cd A⁻¹, a maximum power efficiency of 32 lm W⁻¹ and a maximum EQE of 15.7%. Noticeably, the device A showed superior blue color purity than device D with the CIE coordinate of (0.15, 0.30).

4. Conclusion

In summary, three new iridium compounds have been synthesized and investigated by introduction the F, Cl and Br atoms to the 4-position of pyridine ring in Flrpic. The introduction of F atom on the pyridine ring enlarged

the HOMO–LUMO gap of Flrpic by decreasing the HOMO level while keeping the LUMO of Flrpic almost undisturbed, which consequently resulted in the blue-shift emission of Flrpic. This observation broke the widely recognition that electron-withdrawing F atom is supposed to lower the LUMO energy level. On the other hand, the addition of Cl and Br atoms narrowed the HOMO–LUMO gap of Flrpic and caused the emission red-shift by simultaneously stabilizing both the HOMO and LUMO levels of Flrpic. These iridium compounds exhibited good performance in PhOLEDs. The 4-Cl-Flrpic-based device achieved a maximum current efficiency of 39 cd A⁻¹, a maximum power efficiency of 41 lm W⁻¹ and a maximum EQE of 16% with a bluish-green CIE coordinate of (0.18, 0.40). Remarkably, the 4-F-Flrpic-based device achieved a maximum current efficiency of 29 cd A⁻¹, a maximum power efficiency of 29 lm W⁻¹ and a maximum EQE of 14.6% with a satisfactory blue CIE coordinate of (0.15, 0.28). We believe that the device efficiencies would get improved with suitable bipolar host materials.

Acknowledgments

We are grateful to the National Basic Research Program of China (973 Program 2013CB834805, 2009CB623602 and 2009CB930603), the National Science Fund for Distinguished Young Scholars of China (No. 51125013), and the Fundamental Research Funds for the Central Universities of China.

Appendix A. Supplementary material

Supplementary data associated with this article can be found, in the online version, at <http://dx.doi.org/10.1016/j.orgel.2013.09.026>.

References

- [1] (a) M.A. Baldo, D.F. O'Brien, Y. You, A. Shoustikov, M.E. Thompson, S.R. Forrest, *Nature* 395 (1998) 151; (b) Y. Tao, Q. Wang, C. Yang, Q. Wang, Z. Zhang, T. Zou, J. Qin, D. Ma, *Angew. Chem. Int. Ed.* 47 (2008) 8104.
- [2] H. Sasabe, J.-I. Takamatsu, T. Motoyama, S. Watanabe, G. Wagenblast, N. Langer, O. Molt, E. Fuchs, C. Lennartz, J. Kido, *Adv. Mater.* 22 (2010) 5003; (b) R. Wang, D. Liu, H. Ren, T. Zhang, H. Yin, G. Liu, J. Li, *Adv. Mater.* 23 (2011) 2823; (c) L. Chen, C. Yang, J. Qin, J. Gao, H. You, D. Ma, *J. Organomet. Chem.* 691 (2006) 3519; (d) C.-L. Ho, W.-Y. Wong, *New J. Chem.* 37 (2013) 1665.
- [3] (a) C. Fan, F. Zhao, P. Gan, S. Yang, T. Liu, C. Zhong, D. Ma, J. Qin, C. Yang, *Chem.-Eur. J.* 18 (2012) 5510; (b) L. Chen, H. You, C. Yang, D. Ma, J. Qin, *Chem. Commun.* (2007) 1352; (c) C.-H. Yang, M. Mauro, F. Polo, S. Watanabe, I. Muenster, R. Fröhlich, L. De Cola, *Chem. Mater.* 24 (2012) 3684.
- [4] (a) Y. Chi, P.-T. Chou, *Chem. Soc. Rev.* 39 (2010) 638; (b) L. Xiao, Z. Chen, B. Qu, J. Luo, S. Kong, Q. Gong, J. Kido, *Adv. Mater.* 23 (2011) 926; (c) W.-Y. Wong, C.-L. Ho, *J. Mater. Chem.* 19 (2009) 4457; (d) G. Zhou, W.-Y. Wong, X. Yang, *Chem. Asian J.* 6 (2011) 1706; (e) Y. Liu, K. Ye, Y. Fan, W. Song, Y. Wang, Z. Hou, *Chem. Commun.* (2009) 3699.
- [5] L. Piela, *Ideas of Quantum Chemistry*, Elsevier, 2007.
- [6] A. Tsuboyama, H. Iwawaki, M. Furugori, T. Mukaide, J. Kamatani, S. Igawa, T. Moriyama, S. Miura, T. Takiguchi, S. Okada, M. Hoshino, K. Ueno, *J. Am. Chem. Soc.* 125 (2003) 12971.
- [7] T. Hofbeck, H. Yersin, *Inorg. Chem.* 49 (2010) 9290.
- [8] H. Yersin, *Highly Efficient OLEDs with Phosphorescent Materials*, Wiley-VCH, Berlin, 2007.
- [9] C. Adachi, R.C. Kwong, P. Djurovich, V. Adamovich, M.A. Baldo, M.E. Thompson, S.R. Forrest, *Appl. Phys. Lett.* 79 (2001) 2082.
- [10] L.-L. Wu, C.-H. Yang, I.-W. Sun, S.-Y. Chu, P.-C. Kao, H.-H. Huang, *Organometallics* 26 (2007) 2017.
- [11] D. Di Censo, S. Fantacci, F. De Angelis, C. Klein, N. Evans, K. Kalyanasundaram, H.J. Bolink, M. Grätzel, M.K. Nazeeruddin, *Inorg. Chem.* 47 (2008) 980.
- [12] R. Ragni, E.A. Plummer, K. Brunner, J.W. Hofstraat, F. Babudri, G.M. Farinola, F. Naso, L. De Cola, *J. Mater. Chem.* 16 (2006) 1161.
- [13] S.-Y. Takizawa, H. Echizen, J.-I. Nishida, T. Tsuzuki, S. Tokito, Y. Yamashita, *Chem. Lett.* 35 (2006) 748.
- [14] S.H. Kim, J. Jang, S.J. Lee, J.Y. Lee, *Thin Solid Films* 51 (2008) 722.
- [15] M. Marín-Suárez, B.F.E. Curchod, I. Tavernelli, U. Rothlisberger, R. Scopelliti, I. Jung, D.D. Censo, M. Grätzel, J.F. Fernández-Sánchez, A. Fernández-Gutiérrez, M.K. Nazeeruddin, E. Baranoff, *Chem. Mater.* 24 (2012) 2330.
- [16] C. Fan, Y. Li, C. Yang, H. Wu, J. Qin, Y. Cao, *Chem. Mater.* 24 (2012) 4581.
- [17] C. Hansch, A. Leo, R.W. Taft, *Chem. Rev.* 91 (1991) 165.
- [18] E. Baranoff, B.F. Curchod, F. Monti, F. Steimer, G. Accorsi, I. Tavernelli, U. Rothlisberger, R. Scopelliti, M. Grätzel, M.K. Nazeeruddin, *Inorg. Chem.* 51 (2012) 799.
- [19] S.J. Yeh, M.F. Wu, C.T. Chen, Y.H. Song, Y. Chi, M.H. Ho, S.F. Hsu, C.H. Chen, *Adv. Mater.* 17 (2005) 285.
- [20] M.J. Frisch, G.W. Trucks, H.B. Schlegel, G.E. Scuseria, M.A. Robb, J.R. Cheeseman, G. Scalmani, V. Barone, B. Mennucci, G.A. Petersson, H. Nakatsuji, M. Caricato, X. Li, H.P. Hratchian, A.F. Izmaylov, J. Bloino, G. Zheng, J.L. Sonnenberg, M. Hada, M. Ehara, K. Toyota, R. Fukuda, J. Hasegawa, M. Ishida, T. Nakajima, Y. Honda, O. Kitao, H. Nakai, T. Vreven, J.A. Montgomery Jr., J.E. Peralta, F. Ogliaro, M. Bearpark, J.J. Heyd, E. Brothers, K.N. Kudin, V.N. Staroverov, R. Kobayashi, J. Normand, K. Raghavachari, A. Rendell, J.C. Burant, S.S. Iyengar, J. Tomasi, M. Cossi, N. Rega, J.M. Millam, M. Klene, J.E. Knox, J. B. Cross, V. Bakken, C. Adamo, J. Jaramillo, R. Gomperts, R.E. Stratmann, O. Yazyev, A.J. Austin, R. Cammi, C. Pomelli, J.W. Ochterski, R.L. Martin, K. Morokuma, V.G. Zakrzewski, G.A. Voth, P. Salvador, J.J. Dannenberg, S. Dapprich, A.D. Daniels, O. Farkas, J.B. Foresman, J.V. Ortiz, J. Cioslowski, D.J. Fox, *Gaussian 09, Revision A.02*, Gaussian Inc., Wallingford, CT, 2009.
- [21] S. Lamansky, P. Djurovich, D. Murphy, F. Abdel-Razzaq, H.-E. Lee, C. Adachi, P.E. Burrows, S.R. Forrest, M.E. Thompson, *J. Am. Chem. Soc.* 123 (2001) 4304.
- [22] A.B. Tamayo, B.D. Alleyne, P.I. Djurovich, S. Lamansky, I. Tsyba, N.N. Ho, R. Bau, M.E. Thompson, *J. Am. Chem. Soc.* 125 (2003) 7377.
- [23] Y.-C. Zhu, L. Zhou, H.-Y. Li, Q.-L. Xu, M.-Y. Teng, Y.-X. Zheng, J.-L. Zuo, H.-J. Zhang, X.-Z. You, *Adv. Mater.* 23 (2011) 4041.
- [24] (a) Z. Wu, L. Wang, G. Lei, Y. Qiu, *J. App. Phys.* 97 (2005) 103105; (b) S. Reineke, K. Walzer, K. Leo, *Phys. Rev. B* 75 (2007) 125328.